HHS Public Access

Author manuscript

Nat Neurosci. Author manuscript; available in PMC 2010 October 01.

Published in final edited form as:

Nat Neurosci. 2010 April ; 13(4): 489–494. doi:10.1038/nn.2499.

SYNAPTIC CORRELATES OF FEAR EXTINCTION IN THE AMYGDALA

Taiju Amano[*], **Cagri T Unal**[*], and **Denis Paré**

Center for Molecular and Behavioral Neuroscience, Rutgers, The State University of New Jersey, Newark, New Jersey 07102

Abstract

Anxiety disorders such as post-traumatic stress are characterized by an impaired ability to learn that cues previously associated with danger no longer represent a threat. However, the mechanisms underlying fear extinction remain unclear. Here we show in rats that extinction is associated with increased levels of synaptic inhibition in fear output neurons of the central amygdala (CEA). This increased inhibition results from a potentiation of fear input synapses to GABAergic intercalated amygdala neurons that project to CEA. Enhancement of inputs to intercalated cells required prefrontal activity during extinction training and involved a higher transmitter release probability coupled to an altered expression profile of ionotropic glutamate receptors. Overall, our results suggest that intercalated cells constitute a promising target for pharmacological treatments aiming to facilitate the treatment of anxiety disorders.

It is commonly believed that understanding the mechanisms underlying fear extinction will ultimately lead to improvements in the treatment of anxiety disorders 1,2. Consistent with this, the approach used by clinicians to treat anxiety disorders is similar to that used to extinguish conditioned fear responses in the laboratory. In both cases, the subject is repeatedly presented with the feared object (or conditioned stimulus, CSt) in the absence of adverse consequences (or unconditioned stimulus, USt), leading to fear extinction.

The main amygdala output for fear responses is the central medial nucleus (CEm). Indeed, amygdala projections to the periaqueductal gray, controlling behavioral freezing 3, originate from CEm 4. On the input side, the lateral amygdala is the main target of thalamic and cortical structures conveying CSt information to the amygdala 5,6. Although the lateral nucleus is a critical site of plasticity for conditioned fear 7,8, it does not project to CEm 9–11. However, it can influence CEm indirectly via the basolateral nucleus (BLA) 9–11.

Correspondence should be sent to: Denis Paré, CMBN, Aidekman Research Center, Rutgers, The State University of New Jersey, 197 University Avenue, Newark, NJ 07102, Phone: 973-353-1080 x3251, Fax: (973) 353-1255, pare@axon.rutgers.edu.

[*]The first two authors contributed equally to this report.

Author Contributions

TA and CTU performed all the electrophysiological experiments and most of the analyses on ITC and CEA cells, respectively. TA performed the behavioral training and CTU scored the behavior. DP designed the experiments, wrote the paper, and contributed to the data analysis.

Competing interests statement

The authors declare that they have no competing financial interests.

Consistent with this, post-training BLA lesions abolish conditioned fear responses 12. However, many neurons in the basolateral complex continue to fire strongly to the CSt after extinction training 13–15, highlighting the central paradox of extinction: how does extinction training block fear expression despite the persistence of CSt-evoked responses in BLA?

BLA can influence CEm via direct glutamatergic projections 9–11,16 and through indirect di-synaptic routes involving the glutamatergic excitation of GABAergic intercalated (ITC) 16 or central lateral (CEl) neurons 9–11 that project to CEm 10,11,16,17. Thus, an increased recruitment of ITC or CEl neurons by BLA inputs about the CSt might account for the reduction of fear expression after extinction despite the persistence of CSt-evoked responses in BLA. Moreover, given that ITC cells receive a strong excitatory projection from the infralimbic cortex 18, a prefrontal region required for the consolidation of extinction 2, the increased recruitment of ITC cells by BLA inputs might depend on infralimbic activity. Thus, the present study was undertaken to test whether extinction training alters the responsiveness of ITC and CEA neurons to BLA inputs and assess whether such changes are dependent on infralimbic activity. We found that extinction is associated with an infralimbic-dependent potentiation of BLA inputs to ITC cells leading to an increased inhibition of fear ouput CEm neurons.

RESULTS

To test whether extinction depends on increased levels of feed-forward inhibition in CEm, we first compared the responses of CEm neurons to BLA inputs (Fig. 1a) in coronal slices of the amygdala obtained from rats that were previously subjected to fear conditioning only (n = 16) vs. rats that were fear conditioned and trained on extinction the next day (n = 14; Fig. 1b). This data was contrasted to that obtained in naïve rats (n = 11) and rats presented with the CSt and USt in an unpaired fashion (n = 10; Fig. 1b). We first describe the behavior of these rats (Fig. 1c) and then analyze how the training procedures affected the responsiveness of CEm neurons to BLA inputs *in vitro* (Fig. 1d,e). In this and subsequent experiments, the individuals carrying out the *in vitro* experiments and scoring the rats' behavior were blind to group identity.

Analysis of percent time spent freezing (Fig. 1c) confirmed that rats from the fear conditioning only (Fig. 1c, black) vs. fear conditioning plus extinction (Fig. 1c, red) groups exhibited nearly identical levels of conditioned freezing by the end of the fear conditioning session (Day 2). Although rats from the unpaired groups (Fig. 1c, blue) did not receive paired CSt-USt presentations on Day 2, they did express significant freezing levels (*paired t-test*, habituation vs. last CSt, $P = 0.002$), which presumably represents contextual freezing. On day 3 in a different context, only rats from the extinction group (Fig. 1c, red) received CSt presentations. We measured freezing in the unpaired or fear conditioned rats during corresponding 30 s periods, revealing significantly higher freezing levels in the extinction group than other groups (ANOVA $F(2,59) = 37.83$, $P = 0.0001$; Bonferroni-corrected post-hoc *t-tests*, $P \leq 0.0001$).

Twenty-four hours after exposure to context B, we anesthetized the rats and prepared coronal sections of their amygdala. We obtained patch recordings from samples of 10–16 CEm cells per group and compared their responsiveness to electrical stimuli delivered at a standard position in BLA (Fig. 1a). We carried out these tests from a membrane potential of −45 mV with the lidocaine derivative QX-314 in the pipette solution to facilitate the measurement of IPSP amplitudes without contamination from spike afterhyperpolizations. We observed significant inter-group differences in the amplitude of BLA-evoked IPSPs (Fig. 1d,e; ANOVA $F(3,40) = 4.823$, $P = 0.006$). Bonferroni-corrected post-hoc *t-tests* revealed that CEm neurons from naïve and fear conditioned rats exhibited IPSPs of significantly lower amplitude than in the extinguished and unpaired groups (Fig. 1d; 400 μA; $P \leq 0.028$). However, IPSPs from extinguished rats were not significantly different from those of the unpaired group ($P = 0.9$) and both were abolished by picrotoxin (Fig. S1). Group differences in IPSP amplitudes were not attributable to variations in the passive properties or GABA-A reversal potentials of CEm neurons since we observed negligible differences along these dimensions (Suppl. Tables 1–2 and Fig. S2).

Although EPSP slopes tended to be higher in CEm neurons from the fear conditioned and extinction groups compared to naïve and unpaired animals, these differences did not reach significance (ANOVA, $F(3,38) = 2.31$, $P = 0.92$; Fig. 1e, inset). However, because we studied these CEm cells at a depolarized level (−45 mV) to facilitate IPSP measurements, the testing conditions were not optimal to study BLA-evoked EPSPs. We therefore repeated these tests in separate samples of 13–18 CEm neurons (≥ 5 rats/group) from a membrane potential of −70 mV (Fig. 2a). In these conditions, we detected significant inter-group differences in EPSP slopes (ANOVA $F(3,54) = 4.443$, $P = 0.006$). Bonferroni-corrected post-hoc *t-tests* revealed that EPSP slopes in the fear conditioned group were significantly higher than in the naïve ($P = 0.001$) and unpaired ($P = 0.0014$) animals but did not significantly differ from extinguished animals ($P = 0.099$).

To test how these differences in the character of BLA-evoked responses affect the ability of BLA inputs to fire CEm neurons, we next compared the probability that 10 BLA stimuli of fixed intensity (400 μA) would trigger action potentials in CEm cells from the various groups (Fig. 2b–f). We carried out these tests in samples of 10–15 CEm neurons (≥ 5 rats/group) recorded at rest with a control intracellular solution. We observed large differences in spiking probability between the various groups (ANOVA $F(3,46) = 4.033$, $P = 0.014$). In keeping with the analysis of EPSP slopes, Bonferroni-corrected post-hoc *t-tests* revealed that CEm cells from the fear conditioning group had a higher orthodromic responsiveness than in all other groups ($P \leq 0.042$) with no differences among the latter. It should be noted that BLA-evoked orthodromic spikes had a relatively long latency in CEm cells from the fear conditioning group (9.8 ± 0.7 ms), longer than the latency of the IPSP onset in CEm cells from the extinction group (7.2 ± 0.49 ms; Fig. 2b,c, red arrows) studied at −45 mV (Fig. 1d,e).

Thus, overall the above indicates that fear conditioning is associated with an enhancement of BLA-evoked EPSPs that is partially reversed following extinction. In parallel, extinction training causes a marked increase in BLA-evoked inhibition, a property also seen in the unpaired group.

The increased amplitude of BLA-evoked IPSPs in the unpaired group was unexpected because this paradigm is commonly used as a control for non-associative influences in fear conditioning. However, it was previously reported that presenting the CSt and USt in an unpaired fashion transforms the CSt in a conditioned inhibitor 19 or in other words, a safety signal, an observation we confirmed in our experiments (Fig. S3). This implies that treatments such as extinction and conditioned inhibition causing a reduction of fear responsiveness are associated with persistently increased BLA-evoked inhibition in CEm neurons. What is the origin of this enhanced inhibition? In brain slices, there are only two extrinsic sources of GABAergic inputs to CEm: CEl and ITC cells 10. Thus, we next tested whether treatments that induce an increased inhibition of CEm neurons alter the responsiveness of CEl and ITC cells to BLA inputs.

We first compared BLA-evoked EPSPs in CEl cells from the various groups (Fig. 3a–c). There were significant inter-group differences in EPSP amplitudes (ANOVA $F(3,43) = 3.073$, $P = 0.038$, Fig. 3a,b) and slopes (ANOVA $F(3,35) = 9.78$, $P = 0.0001$; Fig. 3c) with CEl neurons from the unpaired group being significantly more responsive to BLA inputs than in all other groups (Bonferroni-corrected post-hoc *t-tests*, $P \leq 0.001$; Suppl. Table 3). Surprisingly however, CEl neurons from rats of the extinction, home cage, and fear conditioned groups displayed similarly lower BLA-evoked EPSP amplitudes and slopes ($P \geq 0.3$; Fig. 3b,c).

To test whether the stronger EPSPs seen in the unpaired group translated into an enhanced ability of BLA inputs to fire CEl neurons, we next compared the orthodromic responsiveness of CEl cells from the various groups using the same approach as for CEm neurons (samples of 8–11 CEl neurons in ≥ 4 rats/group). Paralleling the EPSP analysis, CEl neurons from the unpaired group had a significantly greater orthodromic responsiveness than all other groups (Fig. 3d; ANOVA $F(3,33) = 3.98$, $P = 0.016$, *t-tests*, $P \leq 0.042$).

The above suggests that the stronger inhibition seen in CEm neurons from the unpaired and extinction groups depend on different mechanisms. In unpaired rats, an increased recruitment of CEl neurons by BLA inputs appears to be involved. However, this was not the case in extinguished rats. To test whether the larger inhibition seen in CEm neurons from extinguished rats resulted from an increased recruitment of ITC cells by BLA inputs, we compared BLA-evoked EPSPs in ITC cells from the various groups (Fig. 4a,b and Fig. S4). Here, we added an additional control group (termed “Unpaired + CS”; n = 12) to determine whether repetitive presentations of a previously unpaired CSt would also modify the responsiveness of ITC cells. These animals were treated like those of the Unpaired group on days 1–2 (Fig. 1b) but received 20 unpaired presentations in context B on day 3.

We observed significant inter-group differences in EPSP amplitudes (ANOVA $F(4,66) = 5.3$, $P = 0.001$; Fig. 4a) and slopes (ANOVA $F(4,62) = 3.559$, $P = 0.011$; Fig. 4b). Bonferroni-corrected *post-hoc t-tests* revealed that ITC cells were significantly more responsive to BLA inputs in the extinction group as compared to all other groups ($P \leq 0.018$). Yet, the passive membrane properties of ITC cells did not vary between groups (Suppl. Table 4).

To test whether the stronger EPSPs seen in the extinction group translated into an enhanced ability of BLA inputs to fire ITC neurons, we next compared the orthodromic responsiveness of ITC cells from the various groups using the same approach as for CEA neurons (samples of 11–19 ITC neurons with ≥ 5 rats/group). Paralleling the EPSP analysis, ITC neurons from the extinction group had a significantly greater orthodromic responsiveness than all other groups combined (Fig. 4c; ANOVA $F(4,66) = 5.19$, $P = 0.0011$) with no differences between the latter (*t-tests*, $P \geq 0.09$).

We considered two possible mechanisms for the enhanced responsiveness of ITC cells to BLA inputs in the extinguished group: (1) an enhanced transmitter release probability by BLA axon terminals contacting ITC cells; (2) an altered expression of ionotropic glutamate receptors at BLA inputs to ITC cells. To test the first possibility, in voltage-clamp mode, we compared the effect of paired BLA stimuli (50 ms inter-stimulus interval) and looked for differences in paired-pulse ratio (Fig. 5a) between cells of the extinction group (n = 9) vs. cells from the various control groups (n = 34). The paired-pulse ratio was significantly lower in the extinction group (n = 9) compared to the control cells (*t-test*, $P = 0.036$; Fig. 5a), suggesting that extinction training produces a modest increase in transmitter release probability at BLA synapses onto ITC cells. See Figure S5 for individual groups.

To test whether extinction training is associated with an altered function of ionotropic glutamate receptors at BLA inputs to ITC cells, in the presence picrotoxin (100 μM), we measured the amplitude of BLA-evoked EPSCs at membrane potentials of –80 and 55 mV and expressed the data in the form of a non-NMDA to NMDA ratio (Fig. 5b). This analysis revealed that the non-NMDA to NMDA ratio was drastically enhanced in ITC cells from the extinction group (n = 8, *t-test*, $P < 0.0001$) compared to cells from the control groups (n = 27; see Figure S6 for individual groups). Overall, these results suggest that the enhanced responsiveness of ITC cells in extinguished rats is due to a modest enhancement in transmitter release probability at BLA synapses on ITC cells and an altered expression profile or phosphorylation level of ionotropic glutamate receptors in ITC cells, in favor of non-NMDA receptors.

Finally, to test whether infralimbic inputs are required for the extinction-related facilitation of BLA inputs onto ITC cells, we compared the amplitude of BLA-evoked EPSPs in rats that received infusions of either vehicle or the GABA-A receptor agonist muscimol in the infralimbic cortex 10 min before extinction training (Fig. 6a and Fig. S7). ITC cells from the muscimol group had a significantly lower responsiveness to BLA inputs than in the vehicle group (Fig. 6b; *t-test*, $P = 0.011$). ITC cells from the muscimol group were indistinguishable from the unpaired control group described above (*t-test*, $P = 0.51$). Similarly, the non-NMDA to NMDA ratio of ITC cells in the muscimol group was significantly lower than in the vehicle group (Fig. 6c,d, $P = 0.0012$), but identical to that of the unpaired group ($P = 0.88$). Overall, these results suggest that the extinction-related changes in the efficacy of BLA-to-ITC synapses are critically dependent on infralimbic activity during and/or shortly after extinction training.

DISCUSSION

This study aimed to shed light on the mechanism underlying the extinction of conditioned fear responses. The interest of this question stems from the fact that some human anxiety disorders such as post-traumatic stress are associated with an extinction deficit20. As a result, understanding the mechanisms of extinction might lead to improvements in the treatment of anxiety disorders. The major findings of the present study are that (1) extinction is associated with increased levels of synaptic inhibition in CEm fear output neurons, (2) this increased CEm inhibition is associated with a potentiation of BLA inputs to ITC cells with GABAergic projections to CEm, (3) this potentiation depends on a higher transmitter release probability and an altered expression profile or phosphorylation level of ionotropic glutamate receptors at BLA synapses onto ITC cells, (4) the extinction-related enhancement in the efficacy of BLA inputs to ITC cells is critically dependent on activity in the infralimbic cortex during extinction training. Below, we consider the significance of these findings in light of previous behavioral and physiological studies on extinction.

Reduced levels of conditioned fear are associated with increased amounts of BLA-evoked inhibition in fear output CEm neurons

Despite years of investigations, there is still uncertainty regarding the nature of CEA control over conditioned fear. CEm output neurons are thought to be GABAergic raising the following question: are conditioned fear responses generated by an increase or a decrease in the CSt-evoked responses of CEm neurons? One study in rabbits21, reported that fear conditioning reduces the CSt-responsiveness of CEA neurons with physiologically-identified projections to the brainstem. In contrast, two other studies, in rats (C.E. Chang, J. D. Berke & S. Maren, *Soc. Neurosci. Abstr.* 478.14, 2008) and mice (S. Ciocchi, C. Herry, C. Muller & A. Luthi, *FENS Abstr.* 4:057.10, 2008), reported the opposite. However, the latter conclusion is supported by the results of stimulation, lesion, and inactivation studies where procedures that increased or decreased CEA activity were generally found to cause augmented or reduced fear expression, respectively3.

The present study provides additional support for this notion. Indeed, we observed that treatments such as extinction and conditioned inhibition, causing a reduction in fear responsiveness, are associated with persistently increased levels of BLA-evoked inhibition in CEm neurons (Fig. S8). However, different populations of GABAergic neurons were responsible for this increased inhibition in conditioned inhibition vs. extinction. In conditioned inhibition (Fig. S8a), the BLA responsiveness of CEl but not ITC neurons was increased relative to that seen in fear conditioned and naïve animals whereas in extinction (Fig. S8b), BLA stimuli elicited stronger responses in ITC but not CEl neurons. The cell type-specific alterations in BLA responsiveness seen as a function of group identity suggest that changes in neuronal excitability at the stimulation site are not responsible for our results. Consistent with this, *ex vivo* studies that examined how prior training on fear conditioning alone, fear conditioning and extinction, or unpaired presentations of the CSt and USt found no significant training-related change in the input resistance of BLA neurons (see 22).

Mechanisms underlying the increased inhibition of CEm neurons following extinction

The finding that BLA stimuli elicit more inhibition in CEm neurons of extinguished than naïve or fear conditioned rats is consistent with earlier results indicating that extinction depends, at least in part, on the strengthening of an inhibitory process23. Several factors suggest that ITC neurons are critical contributors to this increased inhibition. First, ITC cell masses contain one dominant cell type that uses GABA as a transmitter and they project to CEm10,24,25. Second, it was previously shown that the inhibition elicited by BLA stimuli in CEm neurons is blocked by prior pressure application of non-NMDA receptor antagonists in ITC cell clusters16. Last, ITC lesions 26 or pharmacological inhibition of BLA inputs to ITC cells 27 interfere with extinction.

In principle, several pre- and post-synaptic mechanisms could lead to an enhanced inhibition of CEm neurons by BLA inputs. Besides, the increased efficacy of BLA synapses onto ITC cells, as shown here, there could be a facilitation of GABA release by ITC cells themselves, an increased expression or altered phosphorylation state of GABA-A receptor sub-units in CEm neurons, and/or a change in intracellular chloride homeostasis in CEm cells. At odds with this last possibility however, the reversal potential of IPSPs elicited in CEm neurons by pressure application of a GABA-A agonist did not differ between extinguished vs. fear conditioned animals. However, there is evidence of postsynaptic contributions to the enhanced inhibition of CEm neurons in extinction. Indeed, it was reported that extinction training causes an increase in the expression of alpha 2 GABA-A receptor sub-units in CEA28. Thus, these considerations suggest that extinction likely engages a variety of control mechanisms to regulate fear expression.

How could extinction facilitate the recruitment of ITC cells by CSt-related BLA inputs? Extinction was shown to depend on NMDA-dependent synaptic plasticity in the amygdala29–31. Moreover, stimulation of the infralimbic cortex, which sends a robust glutamatergic projection to ITC cells 18, accelerates extinction 32 and inhibit CEm neurons 33. These observations, coupled to the fact that BLA inputs to ITC cells undergo NMDA-dependent long-term potentiation when paired with sufficient depolarization 34, suggest that convergence of BLA and infralimbic inputs to ITC cells during extinction training leads to the NMDA-dependent potentiation of BLA inputs to ITC cells. As a result, the GABAergic output of ITC cells onto CEm neurons would be increased, leading to a reduction of conditioned fear. Given recent data indicating that infralimbic neurons exhibit increased bursting and CSt-evoked responses following extinction training 32,35, plasticity in ITC cells might be further facilitated after extinction training, during a consolidation phase.

Conclusions

Overall, our results suggest that extinction depends, at least in part, on an increased inhibition of fear output CEm neurons. This increased inhibition is caused by an enhanced recruitment of ITC cells by BLA inputs. Moreover, these changes require infralimbic activity during extinction training, suggesting that the infralimbic cortex drives extinction-related plasticity in the amygdala. Since some anxiety disorders are associated with an extinction deficit 20 and hypoactivity of the infralimbic cortex 36,37, our results suggest that

pharmacological manipulations that enhance the excitability of ITC cells by exploiting their unusual profile of receptor expression38,39 could prove useful for treating anxiety disorders.

METHODS

All procedures were approved by the Institutional Animal Care and Use Committee of Rutgers State University, in compliance with the Guide for the Care and Use of Laboratory Animals (Department of Health and Human Services).

Behavior

We used Coulbourn (Allentown, PA) conditioning chambers (25×29×28 cm, with aluminum and Plexiglas walls). Their appearance was altered by introducing various sensory clues. For context-A, we used the chamber described above. For context-B, we introduced a black plexiglass floor washed with peppermint soap in the chamber. The conditioning chambers were placed in sound attenuating boxes with a ventilation fan, and a single house light. Male Sprague-Dawley rats (4–6 weeks old) were randomly assigned to one of five groups. *Naive group*: these rats were left in their home cage until the electrophysiological experiment. On day 1, rats belonging to the other four groups underwent habituation to the training chamber (Context-A) for 20 min. *Fear conditioned group*: on day 2, these rats were presented with 4 tone CSt (4 kHz, 80 dB, 30 s), each co-terminating with a footshock (USt, 0.5 mA, 1 s). The inter-trial intervals were pseudo-randomly drawn from intervals ranging between 80–180 sec (in 10 sec increments). On day 3, they were placed in Context-B but were not presented the CSt or USt. *Extinction group*: these animals were treated like the fear conditioned animals with the exception that on Day 3, they received 20 CSt presentations in context-B. *Unpaired group*: These animals were treated like the fear conditioned animals with the exception that the CSt and USt presentations on Day 2 were unpaired. *Unpaired + CS group*: These rats were treated like the unpaired rats with the exception that on day 3, they received 20 unpaired CSts in context-B.

In a separate experiment, two other rat groups were implanted with infusion cannulas just above the infralimbic cortex under isoflurane anesthesia and in sterile conditions. After recovery, they underwent the same protocol as the extinction animals with the exception that 10 minutes prior to extinction training, they received infralimbic infusions of vehicle (0.2 μl per hemisphere) or muscimol (0.02 μg/0.2 μl).

The behavior of the rats was recorded with a video camera mounted on top of the conditioning chambers. The conditioned response we monitored was behavioral freezing, quantified off-line by an observer blind to the rats' condition. In all groups, the electrophysiological experiments were conducted on day 4.

Electrophysiology

The animals were deeply anesthetized with ketamine, xylazine, and pentobarbital (80, 12, and 60 mg/kg, i.p., respectively). The brain was extracted and cut in 400 μm-thick slices in ice-cold oxygenated artificial cerebrospinal fluid (aCSF) with a vibrating microtome. The aCSF contained (in mM): 126 NaCl, 2.5 KCl, 1.25 NaH_2PO_4, 1 $MgCl_2$, 2 $CaCl_2$, 26 $NaHCO_3$, and 10 glucose, pH 7.3, 300 mOsm. Prior to recordings, slices were kept in an

oxygenated chamber for at least 1h at 24°C, then transferred one at a time to a recording chamber perfused with oxygenated aCSF at a rate of 7 ml/min. The temperature of the chamber was gradually increased to 32°C before the recordings began. Whole-cell patch recordings were performed under visual control with pipettes (6–10 MΩ) pulled from borosilicate glass capillaries and filled with a solution containing (in mM): 130 K-gluconate, 10 N-2-hydroxyethylpiperazine-N'-2-ethanesulfonic acid, 10 KCl, 2 $MgCl_2$, 2 ATP-Mg, and 0.2 GTP-tris(hydroxymethyl) aminomethane (pH 7.2, 280 mOsm) and 0.2% neurobiotin for post-hoc morphological identification of recorded cells and ascertain whether the recordings were obtained from the intended amygdala nucleus. To minimize inter-animal variability in the position of stimulation and recording sites, the following precautions were taken. First, a strict coronal slicing angle was consistently used. Second, all the experiments were conducted using slices at a particular anteroposterior level where the intra-amygdaloid segment of the stria terminalis clearly delineates CEm. Only two 400 μm slices per hemisphere met this criterion. Using a micrometric graticule, the BLA stimulating electrodes were positioned exactly 500 μm ventrolateral to the BLA-CEA border, centered on the lateromedial extent of the CEA nucleus. All ITC recordings were obtained from the adjacent BLA-CEA border region. All CEm and CEl recordings were obtained in the ventral 400 μm region of these sub-nuclei. Stimulation of the targeted BLA region elicited synaptic responses in all tested ITC and CEA cells. In no instance was there a need to reposition the stimulating electrodes. BLA stimuli (100 μs; 0.05 Hz) were applied in a range of intensities (0.1–0.5 mA) increasing in steps of 0.1 mA. At each intensity, we obtained independent averages of three subthreshold responses. For ITC cells, these tests were carried out at a membrane potential of −70 mV, their GABA-A reversal potential. The same potential was used for CEl neurons. For CEm cells, some of the recordings were performed at a membrane potential of −45 mV to facilitate the measurement of IPSPs. To prevent spiking and contamination of the IPSPs by spike after-hyperpolarizations, the lidocaine derivative QX-314 (10 mM) was added to the intracellular solution in CEm cells. Additional samples of CEm cells were studied at rest or −70 mV. In all cases, measurements of EPSP slopes were performed in the first 2 ms of the responses.

Except for ITC recordings on the non-NMDA to NMDA ratio, all experiments were performed in control aCSF. In experiments on the non-NMDA to NMDA ratio, picrotoxin (100 μM) was added to the aCSF to prevent contamination of responses by GABA-A IPSCs. Responses were elicited from − 80 and + 55 mV in voltage clamp mode. The peak current value at −80 mV was considered the non-NMDA component. The current value at 55 mV 300 ms after the stimulus was considered the NMDA component.

The reversal potential of GABA-A IPSPs was estimated by plotting the amplitude of the IPSPs evoked by pressure-applied isoguvacine (200 μM in aCSF) as a function of membrane potential. Linear fits of the data were then performed with the least-squares method. To study the electroresponsive properties of recorded cells, we applied 500 ms current pulses increasing in steps of 0.02 nA. The input resistance of the cells was estimated in the linear portion of current-voltage plots. The membrane time constant was derived from single exponential fits to voltage responses in the linear portion of current-voltage relations.

Statistical Analyses

Statistical analyses consisted of ANOVAs followed by Bonferonni-corrected *t*-tests. All values are reported as average ± s.e.m.

Histology

At the conclusion of the experiments, slices were placed in a fixative (2% paraformaldehyde and 1% glutaraldehyde in 0.1M phosphate buffer, pH 7.4, PB) overnight. To visualize recorded cells, sections were washed in phosphate buffer saline (PBS, 0.1 M, pH 7.4) and then placed in sodium borohydride (1% in PBS, 20 min), and again washed repeatedly in PBS. They were then incubated for 12 h at 23°C in 1% BSA, 0.3% triton, 1% solutions A and B of ABC kit in PBS, washed in PBS, and immersed in a TRIS buffer (0.05M, pH 7.6; 10 min). Neurobiotin was visualized by incubation in a TRIS buffer containing 10 mM imidazole, 700 μM DAB and 0.3% H_2O_2 for 8–10 min. For the infralimbic experiments, thionin-stained coronal sections at the level of the infusion sites were prepared. We only considered data obtained in rats where the infusion cannulas reached the infralimbic cortex. To assess muscimol diffusion, a separate group of 9 deeply anesthetized rats (pentobarbital, 80 mg/kg, ip) were infused with fluorescent muscimol using the same volume and muscimol concentration as in the physiological experiments. Ten minutes later, they were perfused-fixed as above. These controls revealed that with the parameters used here, muscimol remained confined to the infralimbic cortex, diffusing ≤ cubic mm from the center of the infusion site.

Supplementary Material

Refer to Web version on PubMed Central for supplementary material.

Acknowledgements

This material is based upon work supported by NIMH grant RO1 MH083710 to Denis Paré.

REFERENCES AND NOTES

1. Myers KM, Davis M. Mechanisms of fear extinction. Mol. Psychiatry. 2007; 12:120–150. [PubMed: 17160066]
2. Quirk GJ, Mueller D. Neural mechanisms of extinction learning and retrieval. Neuropsychopharmacology. 2008; 33:56–72. [PubMed: 17882236]
3. Davis, M. The role of the amygdala in conditioned and unconditioned fear and anxiety. In: Aggleton, JP., editor. The Amygdala: a functional analysis. Oxford: Oxford University Press; 2000. p. 213-287.
4. Hopkins DA, Holstege G. Amygdaloid projections to the mesencephalon, pons and medulla oblongata in the cat. Exp. Brain Res. 1978; 32:529–547. [PubMed: 689127]
5. LeDoux JE, Cicchetti P, Xagoraris A, Romanski LM. The lateral amygdaloid nucleus: sensory interface of the amygdala in fear conditioning. J. Neurosci. 1990; 10:1062–1069. [PubMed: 2329367]
6. Romanski LM, LeDoux JE. Information cascade from primary auditory cortex to the amygdala: cortex in the rat. Cereb. Cortex. 1993; 3:515–532. [PubMed: 7511012]
7. Amorapanth P, LeDoux JE, Nader K. Different lateral amygdala outputs mediate reactions and actions elicited by a fear-arousing stimulus. Nat. Neurosci. 2000; 3:74–79. [PubMed: 10607398]

8. Maren S, Yap SA, Goosens KA. The amygdala is essential for the development of neuronal plasticity in the medial geniculate nucleus during auditory fear conditioning in rats. J. Neurosci. 2001; 21:RC135. [PubMed: 11245704]
9. Krettek JE, Price JL. A description of the amygdaloid complex in the rat and cat with observations on intra-amygdaloid axonal connections. J. Comp. Neurol. 1978; 178:255–280. [PubMed: 627626]
10. Paré D, Quirk GJ, LeDoux JE. New vistas on amygdala networks in conditioned fear. J. Neurophysiol. 2004; 92:1–9. [PubMed: 15212433]
11. Pitkänen A, Savander V, LeDoux JE. Organization of intra-amygdaloid circuitries in the rat: an emerging framework for understanding functions of the amygdala. Trends Neurosci. 1997; 20:517–523. [PubMed: 9364666]
12. Anglada-Figueroa D, Quirk GJ. Lesions of the basal amygdala block expression of conditioned fear but not extinction. J. Neurosci. 2005; 25:9680–9685. [PubMed: 16237172]
13. Herry C, et al. Switching on and off fear by distinct neuronal circuits. Nature. 2008; 454:600–606. [PubMed: 18615015]
14. Hobin JA, Goosens KA, Maren S. Context-dependent neuronal activity in the lateral amygdala represents fear memories after extinction. J. Neurosci. 2003; 23:8410–8416. [PubMed: 12968003]
15. Repa JC, et al. Two different lateral amygdala cell populations contribute to the initiation and storage of memory. Nat. Neurosci. 2001; 4:724–731. [PubMed: 11426229]
16. Royer S, Martina M, Paré D. An inhibitory interface gates impulse traffic between the input and output stations of the amygdala. J. Neurosci. 1999; 19:10575–10583. [PubMed: 10575053]
17. Petrovich GD, Swanson LW. Projections from the lateral part of the central amygdalar nucleus to the postulated fear conditioning circuit. Brain Res. 1997; 763:247–254. [PubMed: 9296566]
18. McDonald AJ, Mascagni F, Guo L. Projections of the medial and lateral prefrontal cortices to the amygdala: A Phaseolus vulgaris leucoagglutinin study in the rat. Neuroscience. 1996; 71:55–75. [PubMed: 8834392]
19. Rescorla RA. Conditioned inhibition of fear resulting from negative CS-US contingencies. J. Comp. Physiol. Psychol. 1969; 67:504–509. [PubMed: 5787403]
20. Milad MR, et al. Presence and acquired origin of reduced recall for fear extinction in PTSD: results of a twin study. J. Psychiatr. Res. 2008; 42:515–520. [PubMed: 18313695]
21. Pascoe JP, Kapp BS. Electrophysiological characteristics of amygdaloid central nucleus neurons during Pavlovian fear conditioning in the rabbit. Behav. Brain Res. 1985; 16:117–133. [PubMed: 4041212]
22. Lin HC, Mao SC, Gean PW. Block of gamma-aminobutyric acid-A receptor insertion in the amygdala impairs extinction of conditioned fear. Biol. Psychiatry. 2009; 66:665–673. [PubMed: 19482263]
23. Harris JA, Westbrook RF. Evidence that GABA transmission mediates contextspecific extinction of learned fear. Psychopharmacology (Berl.). 1998; 140:105–115. [PubMed: 9862409]
24. Paré D, Smith Y. Distribution of GABA immunoreactivity in the amygdaloid complex of the cat. Neuroscience. 1993; 57:1061–1076. [PubMed: 8309543]
25. Paré D, Smith Y. The intercalated cell masses project to the central and medial nuclei of the amygdala in cats. Neuroscience. 1993; 57:1077–1090. [PubMed: 8309544]
26. Likhtik E, Popa D, Apergis-Schoute J, Fidacaro GA, Pare D. Amygdala intercalated neurons are required for expression of fear extinction. Nature. 2008; 454:642–645. [PubMed: 18615014]
27. Jungling K, et al. Neuropeptide S-mediated control of fear expression and extinction: role of intercalated GABAergic neurons in the amygdala. Neuron. 2008; 59:298–310. [PubMed: 18667157]
28. Heldt SA, Ressler KJ. Training-induced changes in the expression of GABAA-associated genes in the amygdala after the acquisition and extinction of Pavlovian fear. Eur. J. Neurosci. 2007; 26:3631–3644. [PubMed: 18088283]
29. Falls WA, Miserendino MJD, Davis M. Extinction of fear-potentiated startle: blockade by infusion of an NMDA antagonist into the amygdala. J. Neurosci. 1992; 12:854–863. [PubMed: 1347562]
30. Lee H, Kim JJ. Amygdalar NMDA receptors are critical for new fear learning in previously fear-conditioned rats. J. Neurosci. 1998; 18:8444–8454. [PubMed: 9763487]

31. Walker DL, Ressler KJ, Lu KT, Davis M. Facilitation of conditioned fear extinction by systemic administration or intra-amygdala infusions of D-Cycloserine as assessed with fear-potentiated startle in rats. J. Neurosci. 2002; 22:2343–2351. [PubMed: 11896173]

32. Milad MR, Quirk GJ. Neurons in medial prefrontal cortex signal memory for fear extinction. Nature. 2002; 420:70–74. [PubMed: 12422216]

33. Quirk GJ, Likhtik E, Pelletier JG, Pare D. Stimulation of medial prefrontal cortex decreases the responsiveness of central amygdala output neurons. J. Neurosci. 2003; 23:8800–8807. [PubMed: 14507980]

34. Royer S, Pare D. Bidirectional synaptic plasticity in intercalated amygdala neurons and the extinction of conditioned fear responses. Neuroscience. 2002; 115:455–462. [PubMed: 12421611]

35. Burgos-Robles A, Vidal-Gonzalez I, Santini E, Quirk GJ. Consolidation of fear extinction requires NMDA receptor-dependent bursting in the ventromedial prefrontal cortex. Neuron. 2007; 53:871–880. [PubMed: 17359921]

36. Bremner JD, Elzinga B, Schmahl C, Vermetten E. Structural and functional plasticity of the human brain in posttraumatic stress disorder. Prog. Brain Res. 2008; 167:171–186. [PubMed: 18037014]

37. Shin LM, Rauch SL, Pitman RK. Amygdala, medial prefrontal cortex, and hippocampal function in PTSD. Ann. N. Y. Acad. Sci. 2006; 1071:67–79. [PubMed: 16891563]

38. Herkenham M, Pert CB. Light microscopic localization of brain opiate receptors: a general autoradiographic method which preserves tissue quality. J. Neurosci. 1982; 2:1129–1149. [PubMed: 6286904]

39. Jacobsen KX, Hoistad M, Staines WA, Fuxe K. The distribution of dopamine D1 receptor and mu-opioid receptor 1 receptor immunoreactivities in the amygdala and interstitial nucleus of the posterior limb of the anterior commissure: relationships to tyrosine hydroxylase and opioid peptide terminal systems. Neuroscience. 2006; 141:2007–2018. [PubMed: 16820264]

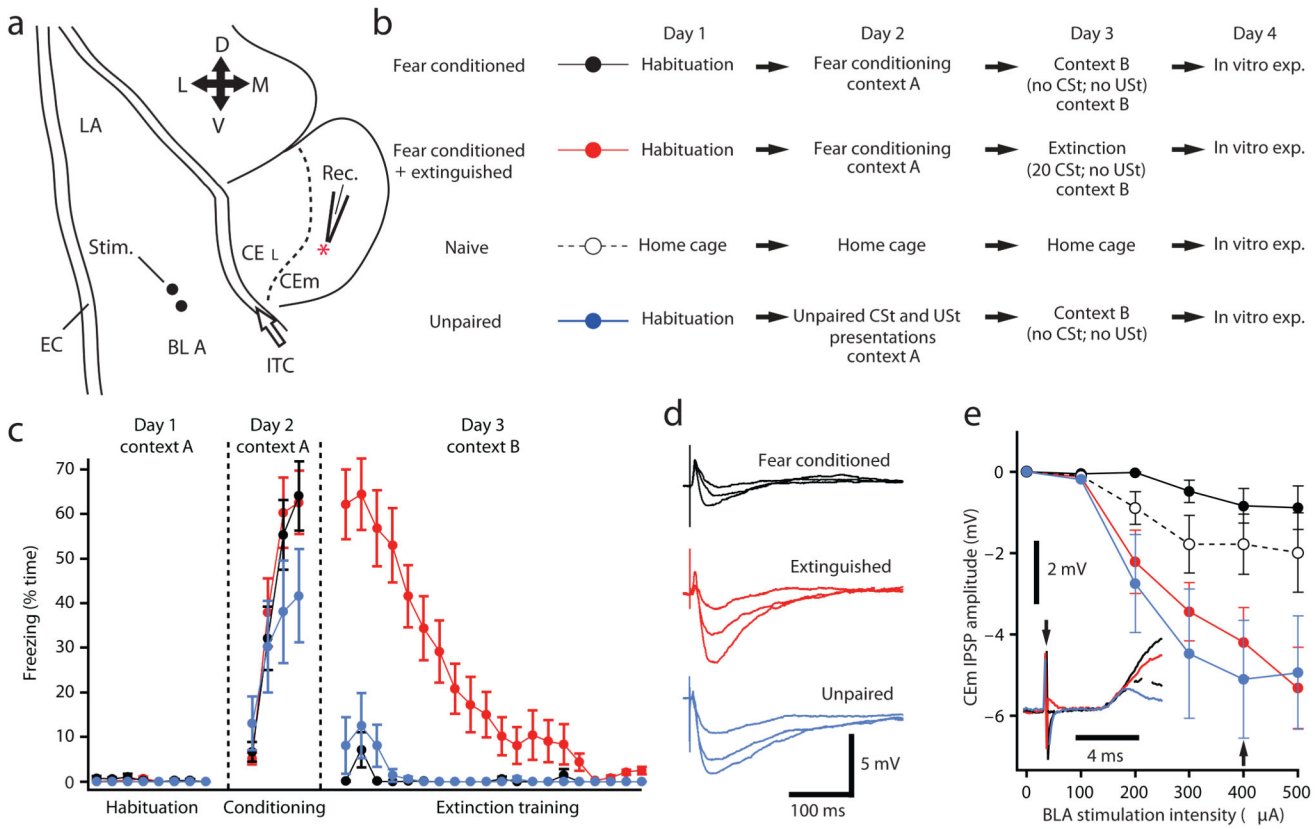

Fig. 1.

Increased inhibition of CEm neurons in extinction and conditioned inhibition. (**a**) Experimental set-up. (**b**) Control and experimental groups. (**c**) Proportion of time spent freezing (average ± s.e.m.) during the various phases of the behavioral protocol (x-axis). During habituation, no CSt was presented and the values show % freezing during randomly selected 30-s periods. During the conditioning phase, all groups were presented with 4 CSts but they were paired with footshocks only in the “Fear conditioning” (black) and “Fear Conditioning plus extinguished” (red) groups. Nevertheless, for all groups, the data shows % time freezing during the CSt. During the extinction training phase, the “Fear conditioning” (black) and “Unpaired” (blue line and filled circles) groups were not presented with the CSt. Thus, we provide % time spent freezing during corresponding 30-s periods. The “Fear Conditioning plus extinguished” (red) groups were presented with 20 CSts. (**d)** Representative examples of BLA-evoked responses in CEm cells recorded with 10 mM QX-314 in pipette solution. Three superimposed responses elicited by 300, 400, and 500 A BLA stimuli. (**e**) Intensity-dependence of BLA-evoked IPSPs in CEm neurons (average ± s.e.m.). **Inset** in **e** shows rising phase of BLA-evoked EPSPs (400 µA). Number of tested CEm cells: Fear conditioned 16; Extinguished 16; Naïve 12; Unpaired 10.

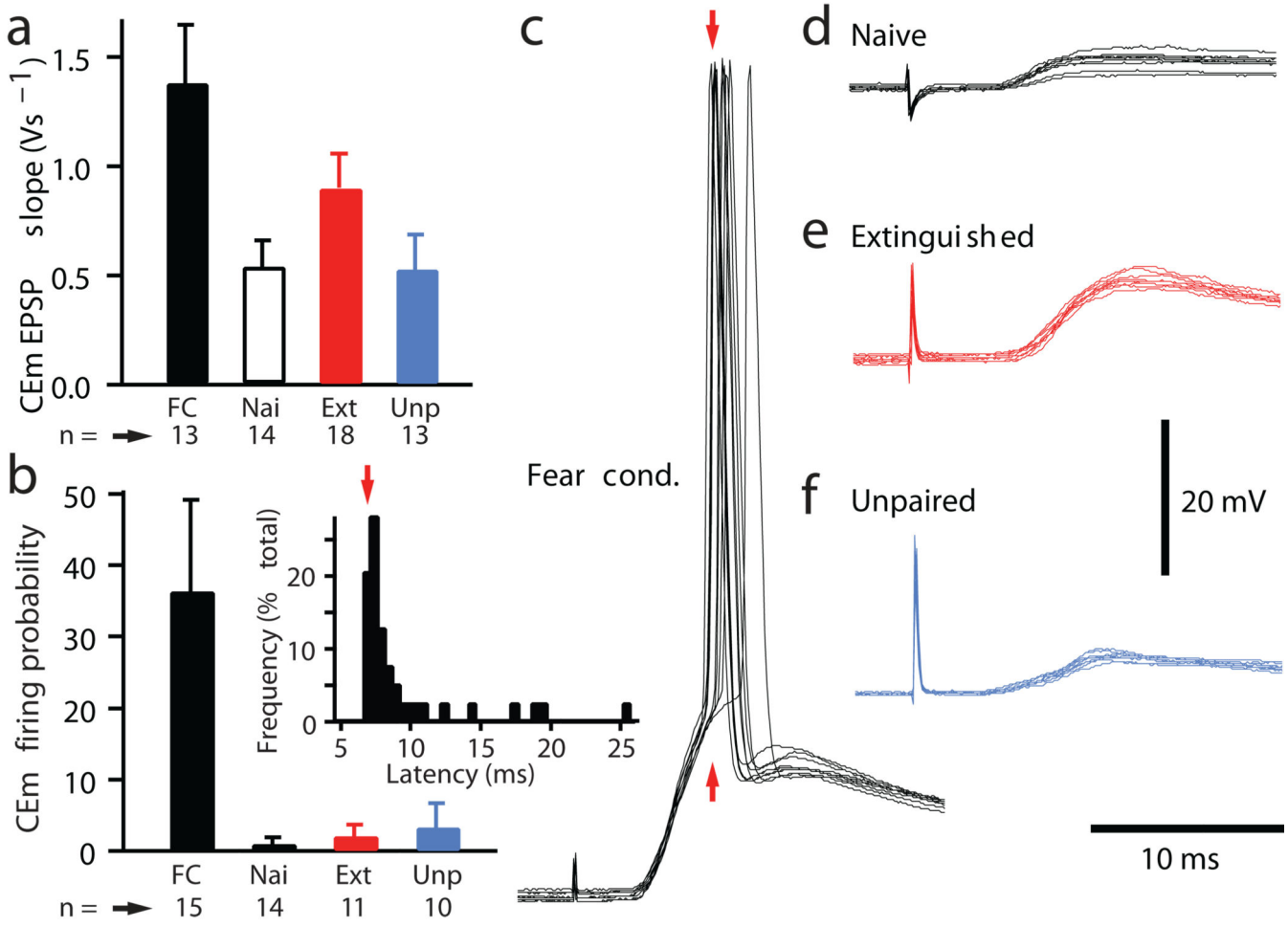

Fig. 2.

Group-related differences in CEm EPSP slopes and orthodromic spiking in response to BLA stimulation. (**a**) Slope of BLA-evoked EPSPs (initial 2 ms; from −70 mV; average ± s.e.m.) and (**b**) percent BLA stimuli (400 μA) eliciting orthodromic spikes (average ± s.e.m.; from rest) in CEm cells from the various groups (x-axes). **Inset**, normalized frequency distribution of BLA-evoked spike latencies in CEm neurons of the fear conditioned group. (**c**–**f**) Representative examples of BLA-evoked responses (10 superimposed stimuli) in CEm cells from the various groups. **Red arrows** indicates average time of EPSP-IPSP transition in CEm cells from the extinction group studied at −45 mV.

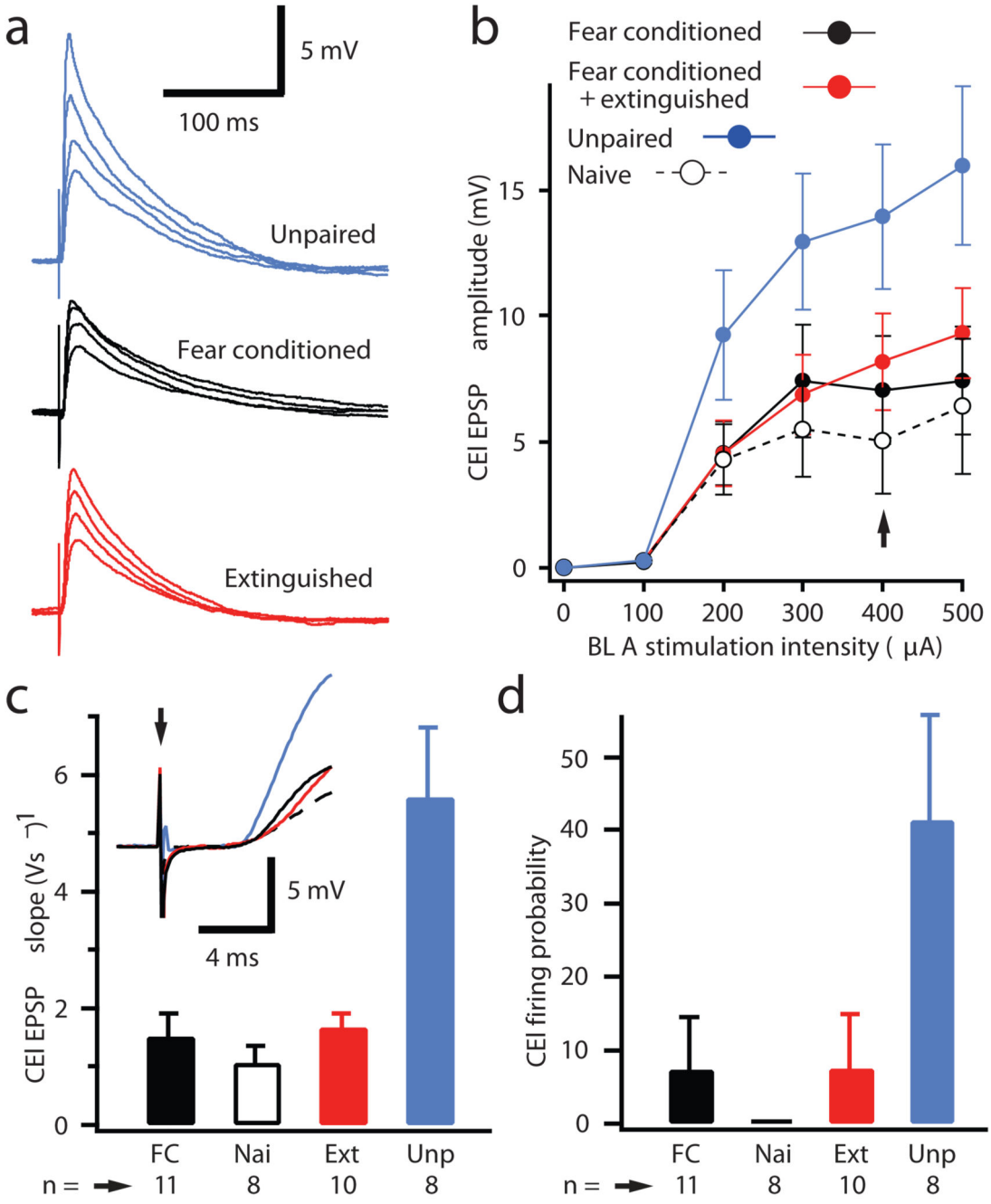

Fig. 3.

Increased recruitment of CEl neurons by BLA inputs in conditioned inhibition. (**a**) Representative examples of BLA-evoked responses in CEl cells in control aCSF. Superimposition of four responses elicited by BLA stimuli of 200–500 µA increasing in 100 A steps. (**b**) Intensity-dependence of BLA-evoked EPSP peak amplitudes in CEl neurons (average ± s.e.m.). Number of tested CEl cells: Fear conditioned 14; Extinguished 14; Naïve 13; Unpaired 14. (**c**) Slope of BLA-evoked (400 µA stimuli) EPSPs (first 2 ms) in CEl neurons from the various groups (average ± s.e.m.). **Inset** shows rising phase of BLA-

evoked EPSPs. (**d**) Percent BLA stimuli (400 μA) eliciting orthodromic spikes from rest (average ± s.e.m.) in CEl cells from the various groups (x-axis).

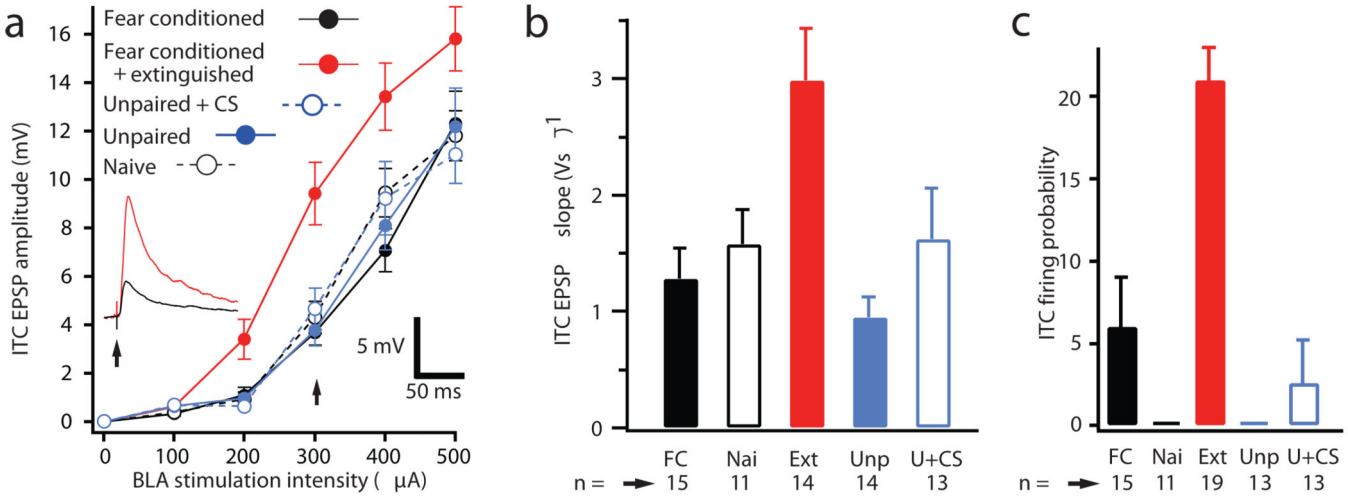

Fig. 4.

Enhanced efficacy of BLA synapses onto ITC cells in extinction. (**a**) Intensity-dependence of BLA-evoked EPSPs in ITC neurons (average ± s.e.m.) in control aCSF. **Inset** shows representative ITC cells from the extinction (red) and fear conditioning (black) groups (300 µA). (**b**) Slope of BLA-evoked (400 µA stimuli) EPSPs (first 2 ms) in ITC neurons from the various groups (average ± s.e.m.). (**c**) Percent BLA stimuli (400 µA) eliciting orthodromic spikes from rest (average ± s.e.m.) in ITC cells from the various groups (x-axis).

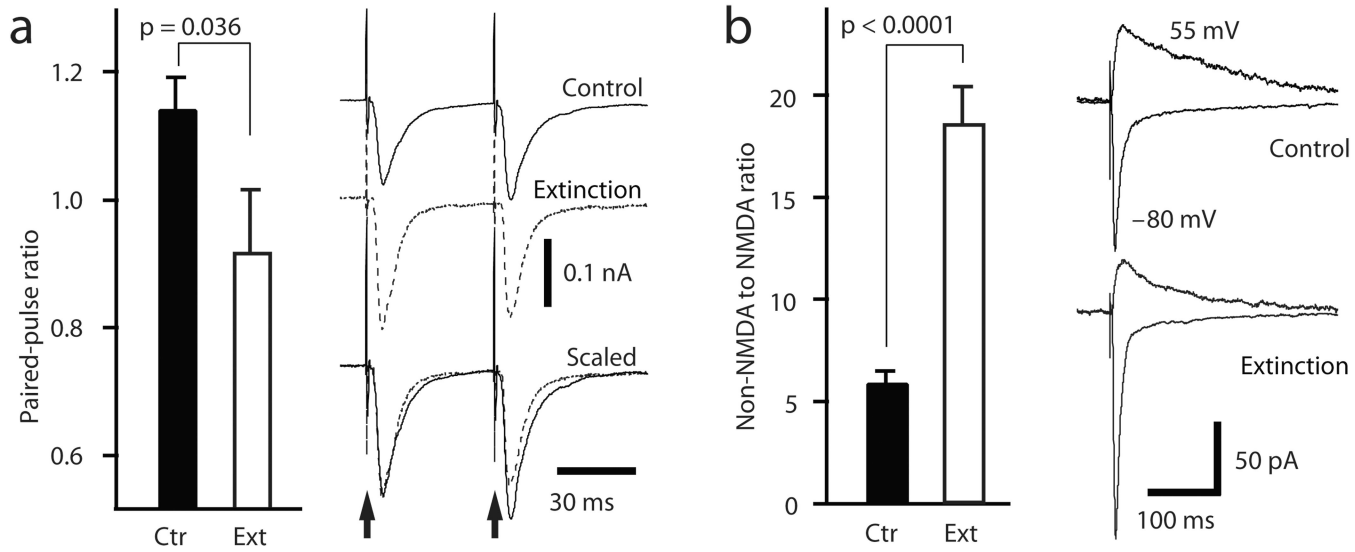

Fig. 5.

Mechanisms underlying increased BLA responsiveness of ITC cells in extinction. (**a**) Histogram on left shows paired pulse ratio (average ± s.e.m.) in ITC cells from the control (n = 34) and extinction (n = 9) groups. Traces on right show representative examples of ITC responses to paired BLA stimuli (50 ms inter-stimulus interval; 500 μA). (**b**) Histogram on left shows Non-NMDA to NMDA ratio (average ± s.e.m.) in ITC cells from the control (n = 27) and extinction (n = 8) groups. Traces on right show representative examples of ITC responses to BLA stimuli (500 μA) at −80 and 55 mV.

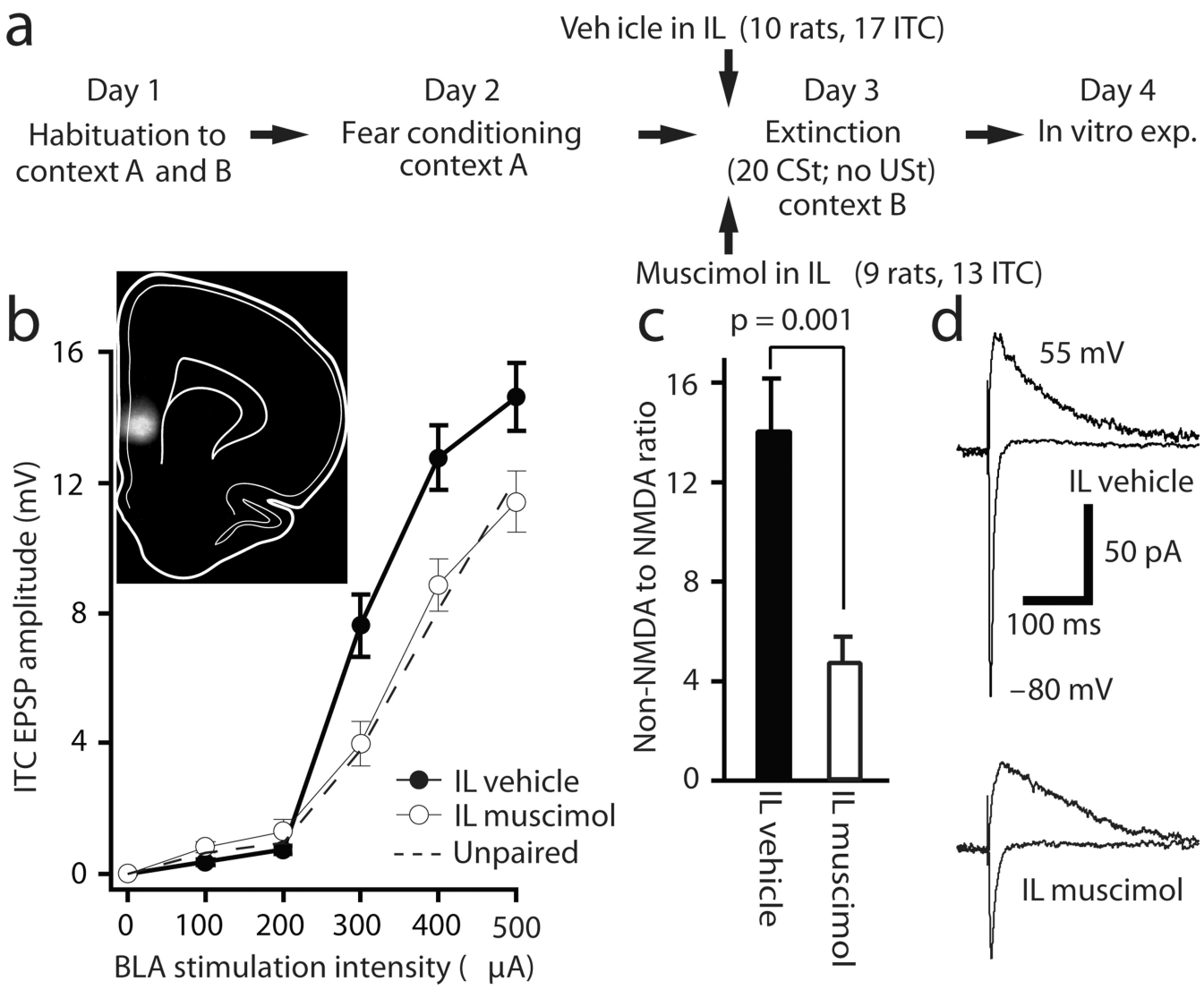

Fig. 6.

Infralimbic (IL) inactivation blocks extinction-related changes in the efficacy of BLA synapses onto ITC cells. (**a**) Experimental paradigm. (**b**) Intensity-dependence of BLA-evoked responses in ITC cells from the vehicle (n = 15) and muscimol (n = 11) groups (average ± s.e.m.). Dashed line indicates data from unpaired group reproduced from figure 2. **Inset** shows extent of fluorophore-conjugated muscimol diffusion in the infralimbic cortex. (**c**) Non-NMDA-to-NMDA ratio (average ± s.e.m.) in ITC cells from the vehicle (n = 9) and muscimol (n = 8) groups. (**d**) Representative examples of ITC responses to BLA stimuli (500 µA) at −80 and 55 mV.